Mine Water Environ
DOI 10.1007/s10230-007-0005-5

TECHNICAL ARTICLE

Geological Analysis and Numerical Modeling of Mine Discharges for the Sanshandao Gold Mine: 2. Simulation and Prediction of Mine Discharges

Chunping Liu · Bo Peng · Jianxin Qin

Received: 31 March 2007 / Accepted: 7 June 2007

Abstract A two-dimensional model is presented as a way to hydrogeologically characterize the controlling factors in the Sanshandao Gold Mine. The finite element method was first applied to simulate the ground water system of the current operation, using leakage data and the calculated recharge. An inverse model was applied to the observed data (e.g., head and discharge) to verify and calibrate the ground water simulation model and to estimate the hydrogeological parameters for the water-bearing zones. Nonlinear mathematic programming was used to solve the inverse model and to estimate the model parameters in 17 districts with different hydrogeological characteristics. The finite element equations were solved by means of a large non-symmetrical sparse equation. The results were in agreement with what is currently observed in the mine. The models and the estimated parameters were then applied to predict the mine water discharge for drifts extending to depths of –330 to –600 m during the next development stage. In order to improve the predicted accuracy of the numerical model, an iterative element mesh was added in the districts near the drainage drifts so that the computed discharges that flowed into the drifts would approach the recharges that flow into the borders of the mine. The model was also used to understand how the mine discharge would be influenced by factors such as unsteady ground water flow and the construction of hydraulic barriers to restrict ground water from entering the pits.

Keywords Ground water simulation · Mine discharge · Parameter estimation · Sanshandao

Introduction

The finite element method (FEM) has been used by many researchers to numerically model ground water movement (e.g., Xu and Zu 1999; Xue et al 1991; Yeh 1981). Numerical modeling of ground water movement generally includes two steps: first, an appropriate inverse problem is formulated and solved, and then, the ground water discharge is predicted using the FEM. Districting or interpolating methods are normally used to solve the inverse problem, but this is almost always difficult because the numerical procedures are neither unique nor stable (Yeh 1986). Compared to the interpolating method, the districting method is simpler and more practical, and is widely used in China (Liu and Zheng 1994; Xu and Zu (1999). Mathematical programming methods such as the gradient method, Newton–Raphson, and Gauss–Newton iteration are alternative ways to approach the inverse problem of ground water models (Chang and Yeh 1976; Larabi and Smedt 1994). A two-dimensional model for a ground water system with sloping and horizontal bases is presented in this paper; it was applied using a technique that is used to solve large non-symmetric sparse equations (Liu et al 1980). A districting inverse problem was formulated by setting a function to minimize the difference between calculated and observed data. Non-linear programming was used to estimate the hydrogeological parameters of the water-bearing zones. During the second development stage, deeper drifts (–330 to –610 m) are planned; discharges of the mine are numerically predicted for these sections using the simulation model, in which the drifts are treated as an

Part 1 of this article can be found at doi:10.1007/s10230-007-0004-6.

C. Liu (✉) · B. Peng · J. Qin
College of Resource and Environment Science,
Hunan Normal University, 410081 Changsha, China
e-mail: lcp62@hotmail.com

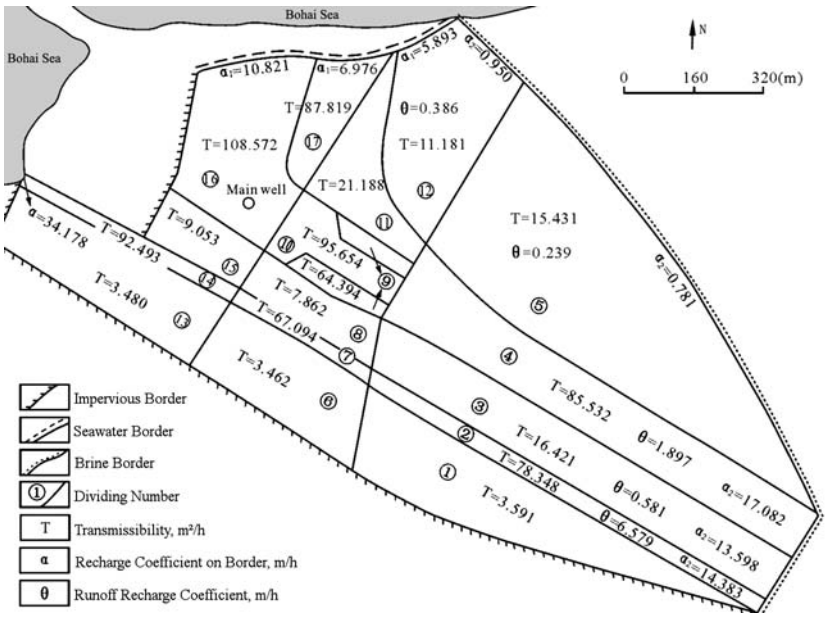

Fig. 5 Sketch showing the parameters estimated in each district of the mine

initial boundary condition with known heads (equal to the drift elevations). Such forecasting involves many complicated factors; some analyses and discussions are presented for some of the factors that will influence the mine discharge, such as the unsteady ground water flow, the base depth of the water-bearing zones, and the emplacement of hydraulic barriers to prevent ground water from entering the pits. This work will now be used to design the drainage system during the second stage of mining.

Model of the Groundwater Movement

Simplification of Hydrogeological Conditions

At present, the hydraulic gradient of ground water is 0.2 in the mine area; it is anticipated to become steeper as pumping increases. According to laboratory results (Xue et al. 1986), at this hydraulic gradient, ground water flow in fissures more than 2 mm wide is normally non-laminar. Although the major fractures in the mine are all wider than this, the fissures are mostly cemented. Therefore, the ground water movement for the whole mine area can be considered as a laminar flow field.

During the first stage of excavation, the ground water movement was unsteady. Since not all of the data from the first stage of development was available, it was difficult to define some of the parameters, such as elastic storativity and specific yield of the water-bearing zones. As the testing time of stopping and then releasing water in zone III_1 and III_3 (see the preceding companion paper) was limited (due to concerns about compromising production activity), it was not possible to acquire the parameters of unsteady flow. During mining, the discharge of seawater into the mine stabilized, while the amount of brine decreased very gradually. Therefore, the ground water movement for the mine was approximated as a steady flow.

The water-bearing zone III is not only the recharge pathway of seawater and brine, but also where ground water discharges to the mine pit. This work models the ground water movement in zone III. The base of the III_1 is defined in Fig. 5; the base of the III_2 and III_3 zones can be regarded as horizontal, with an inferring elevation of –700 m (see Fig. 5 in Liu et al. 2007). Because we hope to establish a two-dimensional model of ground water movement for both the horizontal and slope basement, the *X*-axis of the coordinate system was assumed to align with the base of each water-bearing zone in the southeast direction (i.e., the direction of the exploration line or the dip of the F_1 in plane projection), and the *Y*-axis to be perpendicular to the *X*-axis of each zone in the northeast direction (i.e., the trend of the F_1 in plane projection). This allowed us to simulate the ground water movement as two-dimensional, whether the base is horizontal or sloping.

Modeling the Ground Water Movement

For the ground water system mentioned above, flow can be described by a partial differential equation (Chen 1986):

$$\nabla(\mathrm{T}\nabla\Phi) - \theta\nabla\Phi + R = \sum \delta(x_{\mathrm{w}}, y_{\mathrm{w}})Q_{\mathrm{w}} \qquad (9)$$

where Φ represents drawdown of ground water head; Q_{w} represents the discharge of drainage into the mine pit; θ is the coefficient of brine runoff recharge ($\theta = US$, U is true velocity of brine flow through fissure; S is the elastic storativity of the water-bearing zone); R is recharge density of the Quaternary water (including low mineralized

bedrock water); and $T = KM$, in which K is the coefficient of permeability, and M is the thickness of the aquifer, and has different value for each water-bearing zone:

$$M = \begin{cases} (\Phi - B) & \text{for the III}_2 \text{ and III}_3 \\ (\Phi - B)\cos\beta & \text{for the unconfined zone of the III}_1 \\ m\cos\beta & \text{for the confined zone of the III}_1 \end{cases} \quad (10)$$

where B is the base elevation of the water-bearing zone; m and β is the thickness and sloping angle of the III_1 zone, respectively. In the left of Eq. (9), the second term exists only in the runoff region of brine. Boundary conditions of the ground water flow model are expressed by Eq. (3), (6), and (7) (in Liu et al. (2007), which can be solved by FEM if the parameters in these equations can be determined. It is a nonlinear equation due to the unconfined water term in Eq. (10); the coefficient matrix of finite element equations is asymmetrical due to the runoff recharge term in Eq. (9).

Parameter Estimation

There are three types of hydrogeologic parameters in the above equations, i.e., the transmissivity (T) and runoff recharge coefficient (θ) in Eq. (9), and the boundary coefficients (α_1) and (α_2) in Equations (3), and (6) (in Liu et al (2007). These parameters are defined as the vector of $\lambda = \{T,\theta,\alpha\}$. The water-bearing zones are divided for 17 parameter districts for the mine based on the geological and geophysical data of the characteristics of the fissures. There is one parameter T in each district, one $\alpha(\alpha_1$ or $\alpha_2)$ boundary coefficient in the district that involves the third type of boundary conditions, and one θ in the runoff recharge district of brine. So the total number of parameters that need to be estimated in the model is 17 + 9+5 = 31 (see Fig. 5).

The finite element equation of the groundwater movement for a typical element e can be written as:

$$\sum_e \{\lambda[a]\{\varphi\}^e - \{f\}^e\} = \sum_e \{[Ta_1 + \theta a_2 + \alpha a_3]\{\varphi\}^e - \{f\}^e\} = 0 \quad (11)$$

where e is element number; φ is the head vector of the element; $a = Ta_1+\theta a_2+\alpha a_3$ is the 3×3 coefficient matrix of the element, and a_1, a_2, and a_3 are also the 3×3 coefficient matrix; and f is the free term of the element. The first three terms of Eq. (11) are derived from the first two terms of Eq. (9) and the boundary condition of Eqs. (3) and (6). Given the parameter vector $\lambda = \{T, \theta, \alpha\}$, a system of algebraic equations for the head vector $\{\varphi_1, \varphi_2,\ldots\}$can be obtained by summing the contributions from all elements for e = 1, 2, 3,…

$$[A(\lambda)]\{\varphi\} = F \quad (12)$$

where [A] is the coefficient matrix of the finite element equation. In order to iteratively estimate the hydrogeologic parameters of the mine, a preliminary parameter solution vector λ should be assumed in Eq. (12), and an initial head vect*or* $\{\varphi\}$ can be calculated by substituting the parameter vector λ to Eq. (12); the trial solution vector $\{\lambda, \varphi\}$ is then obtained. Calculating derivatives by using Eq. (11) with respect to the lth parameter λ_l at the trial solution leads to

$$\sum_e [\underline{a}]^e \left\{\frac{\partial\varphi}{\partial\lambda_l}\right\} - \left\{\underline{y}_l\right\}^e = 0 \quad (13)$$

where $\underline{a} = a(\lambda)$ is the coefficient matrix; $\underline{y}^e_{l^e} = [\partial a/\partial\lambda_l]\left\{\underline{\varphi}\right\}^e$ is a 3×1 column vector, and can be calculated by using Eq. (11), for example, $\underline{y}_l = [a_1]\ \{\varphi\}^e$ for $\lambda_1 = T\ i$. Equation (13) can be rewritten by summing the contribution of each element:

$$[A(\underline{\lambda})]\{J_l\} = \underline{Y}_l \quad (14)$$

where, $\underline{Y}_l = [\partial A/\partial\lambda_l]\{\varphi\}$ is a $n \times 1$ column vector; $J_l = \{\partial\varphi_1/\partial\lambda_l\ \partial\varphi_2/\partial\lambda_l\ldots.\ \partial\varphi_n/\partial\lambda_l\ \}$ is the $n \times 1$ *Jocobian* derivative vector of the hydraulic heads at n nodes of the FEM mesh of the mine with respect to parameter λ_l, and has to be determined. For l = 1, 2, …, m, we can set up similar m equation sets with the same coefficient matrix A(λ) and different right term $\underline{Y}_l$ (l = 1,2,…, m). Hence, these equation sets can be simultaneously solved:

$$J_\lambda = [A(\underline{\lambda})]^{-1} Y \quad (15)$$

where, $J_\lambda = \{J_1, J_2, \ldots, J_m\}$ is m column vectors of the n heads (φ_i, i = 1, 2, …, n) with respect to m parameters (λ_l, l = 1, 2, …, m) and $\underline{Y} = \{\underline{Y}_1, \underline{Y}_2, \ldots, \underline{Y}_m\}$ is m column vectors with size $n \times 1$. For the sake of simplicity of the iteration computation, hydraulic head vector $\{\varphi\}$ is expanded by first order Taylor series of Eq. (12) with respect to λ:

$$\varphi = \underline{\varphi} + J_\lambda(\lambda - \underline{\lambda}). \quad (16)$$

Equation (16) is referred to as a response equation for the heads of parameters. In this work, hydro-geologic parameters of the water-bearing zones were finally determined by the optimization model with a minimization objective function f as follows:

$$f = \min\left\{\left[I^T(\varphi - \varphi_c)I\right]^2 + \rho_1(Q^s - Q^s_c)^2 + \rho_2(Q^a - Q^a_c)^2\right\} \quad (17)$$

where I is an $n_w \times 1$ unit column vector, and n_w is the total number of head observed; and φ is the $n_w \times 1$ head column

Table 3 Results of optimal fitting of the head and discharge

Items		Observed values	Calculated values	Error (%)
Head (m)	Well 6	–126.40	–137.37	8.68
	Well 7	–125.90	–120.12	4.59
	Well 8	–90.20	–92.87	2.96
	Well 9	–148.10	–147.51	0.40
	Well 13	–143.60	–142.84	0.53
	Well 15	–199.50	–198.51	0.50
	–150/2,240-1	–111.30	–120.15	7.95
	–150/2,240-2	–129.20	–122.18	5.43
	–240/1,760-12	–186.40	–197.16	5.77
	–240/1,760-14	–184.90	–193.37	4.58
	–240/1,900	–215.10	–203.58	5.36
	–250/1,960-1	–181.90	–192.96	6.08
	–250/1,960-2	–220.10	–207.09	5.91
	–250/1,960-3	–221.00	–208.00	5.88
	–250/2,000	–158.80	–168.11	5.86
	–280/1,900	–184.10	–183.95	0.08
	–280/1,920	–185.90	–177.87	4.02
Discharge (m^3/h)	Seawater	330.5	338.8	2.58
	Brine	170.2	157.3	7.58

vector calculated by response Eq. (16). The subscripts c and o represent calculated and observed values, respectively; Q^s and Q^a are the recharge of seawater and brine entering drifts, respectively; and ρ_1 and ρ_2 are the calculated weight for the recharge of seawater and brine. Once φ is numerically determined, Q^s and Q^a can also be calculated by Darcy's Law.

The above method reflects the hydraulic gradient of ground water for the mine, not only the heads. The constraint conditions of the optimal problem are given by an empirical estimate for the upper and lower limit of parameters in each parameter zone based on the site survey data.

A constrained variable metric algorithm was developed to solve the optimal problem of parameter estimation (Liu 1995). The data utilized in the optimal model include the FEM global mesh of 800 nodes and 1,484 triangle elements, the heads of 11 piezometers in the drifts and 6 observation wells, and the seawater and brine recharge measured on site. The fitting errors for each observation datum are shown in Table 3. The fitting results in Table 3 are basically acceptable; maximum errors occurred at both items of the observation well 6 and brine discharge, with fitting errors of 8.68 and 7.58%, respectively. Well 6 is the brine well located at the southeast at 600 m depth, and its water table changed irregularly, possibly due to problems with the well itself. The fitting error for the brine discharge may be due to a transition from steady to unsteady flow, as the brine discharge gradually decreased with time. The estimated parameters are shown in Fig. 5, and are in agreement with what is currently observed in the mine.

The Forecast Model

Forecast of the Mine Discharge

The mine discharges for the sections of –330 to –610 m drifts planned for the second development stage of the mine were numerically predicted using the previous simulation model in which the drift was treated as a boundary condition with known heads (equal to the drift elevations). The numerical model was again solved using the large non-symmetric sparse equation techniques (Liu et al. 1980). The hydraulic head at each node was then obtained by the iteration of the non-linear equations. Then, Darcy's Law was applied to compute the mining section discharges in different levels of drift.

There were some problems in this calculation process: (1) As the ground water head in the mine decreases, part of the confined water will probably become unconfined water; where this happens, the above-estimated parameters T had to be revised, using the formula: $T = T_0 M/M_0$, where T_0 and M_0 are, respectively, the computed value from the optimal model for transmissibility of water-bearing zones and section height of ground water movement; (2) As the hydraulic gradient increases in the vicinity of the mine pits, a finer element mesh was adopted to improve the computational accuracy. In this work, based on the global mesh, a regional fine mesh of 140 elements and 81 nodes was adopted for the 16×20 m^2 area near the main vertical well; in the calculation process, about 100 additional nodes were added to the element mesh near each horizontal drift. In order to reduce the artificial workload, all newly added nodes and elements were automatically formed and joined to the original finite element mesh; (3) In order to compensate for the effects of 3-dimensional flow, the drainage section in this calculation was chosen at places 20 m away from the drainage drifts.

The calculated discharge was compared with the recharge from the border of the mine (Table 4) to verify the balance between recharge and discharge of the mine during the calculation. The relative errors of the total discharge to recharge in Table 4 tended to increase with increased developed depth, and the forecasted recharges were higher than the discharges for each drift elevation. This may be due to the effect of 3-dimensional flow and the increased mesh density near the pits. Thus, the forecasted recharges are believed to be relatively more accurate than the

Table 4 A comparison of the discharge with the recharge (both in m^3/h)

Drift elevation (m)	–330	–420	–510	–610
Discharge from the main well	218.4	264.1	296.3	319.3
Discharge from drift	441.5	533.8	633.4	740.4
Total discharge	660.0	798.0	929.8	1059.6
Total recharge	685.7	843.2	990.1	1154.4
Relative error (%)	3.88	5.66	6.40	8.94

discharges, and could be used for future drainage design in the mine.

Revising the Predicted Discharge

The mine discharge is influenced by many complicated factors. The following analyses may help in designing the drainage system for the second developmental stage of the mine.

The Effect of Unsteady Flow

The model established in this study was unable to forecast an unsteady discharge. The field observations showed that the water-flow field and the seawater discharge were basically in steady state, but that the discharge of brine decreased slightly with time. That means that the discharge predicted by the model is a bit higher than the actual discharge. On the other hand, the discharge is unsteady due to the release of static storage during mining. According to observations during the first stage of mining, the maximum discharge for the –240 m drift was 650 m^3/h during the unsteady stage, while the discharge during the steady stage was 570 m^3/h. Assuming a linear relationship, the maximum discharge in the mining stage is expected to be 650/570 = 1.14 times that of a steady discharge. Considering that the linear estimate is a bit higher than the actual value, the difference between the maximum and steady discharge is less than 14%. Generally, the result estimated by the above model is higher than the actual discharge during mining (steady flow), but is lower than the maximum discharge (during the initial unsteady flow).

The Effect of Impervious Base Depth

The basement of water-bearing zones in the mine area has not been determined except for the impervious zone III_1, which lies at the bottom of the No.1 altered zone. All the above calculations are based on assuming that the base elevations of the III_2 and III_3 zones are –700 m. In order to test this supposition, a numerical investigation was undertaken to predict the discharge of the –610 m drift. Using different base elevations of –600, –700, –800, –900, and –1000 m, the calculated discharges of –610 m drift are shown in Table 5. The increasing rate of the discharge was 6.94, 3.32, 2.72, and 2.19%, respectively, and correspondingly, the effect of elevation becomes less and less with increased base depth. So it was concluded that the base elevation does not greatly influence the discharge estimate, and that it was reasonable to assume that the basement elevation, B = –700 m in the III_2 and III_3 zones.

The Effect of Ground Water Barriers

The drainage region for the discharge calculation covers the entire distribution spaces of all wells and drifts for the second development stage. In fact, a grout slurry barrier was supposed to be emplaced beyond the ore body zones to enhance safety by decreasing the amount of recharge water. If these plans are implemented before the second stage of mining begins, the calculated discharge for the –610 m drift would be 860 m^3/h, 190 m^3/h less than currently predicted. Thus, the discharge expected by the model ranges from 860 to 1,050 m^3/h, and would have to be adjusted according to the extent and quality of the grouting effort.

Conclusions

The Sanshandao Gold Mine is typical of mines subject to water entering through fractures. Its recharge is controlled by hydrogeological structures that trend northwestward. Seawater and brine are the major recharge sources. Numerical modeling indicates that as mining depth increases, the amount of Quaternary water will decrease but that recharge water will linearly increase due to increased drawdown on the supplemental borders of seawater and

Table 5 The discharge of the –610 m drift changing with basement elevation of the III_2 and III_3 zones

Base elevation of the III_2 and III_3 zones	–600 m	–700 m	–800 m	–900 m	–1000 m
Discharge of –610 m drift	990.79	1059.60	1094.82	1124.58	1149.18
Increasing rate of the discharge (%)	–	6.94	3.32	2.72	2.19

brine. Therefore, it is strongly recommended that hydraulic barriers be emplaced to reduce the amount of mine drainage and increase safety.

Acknowledgments This work was funded by a grant from the Changsha Institute of Mine and was a key project of the Hunan Education Administration.

References

Chang S, Yue WWG (1976) A proposed algorithm for the solution of the large-scale inverse problem in ground water. Water Resour Res 12:365–374

Chen Y (1986) Groundwater movement and water resource evaluation (in Chinese). China Construction Industry Press, Beijing, p 193

Larabi A, Smedt FD (1994) Solving three-dimensional hexahedral finite element ground water models by preconditioned conjugate methods. Water Resour Res 30:509–521

Liu CP (1995) The optimal model of planning and management for ground water system (in Chinese). Zhongnan University Press, Changsha, pp 219–243

Liu CP, Bo P, Jianxin Q (2007) Geological analysis and numerical modeling of mine discharges for the Sanshandao Gold Mine in Shandong, China: 1. Geological Analysis. Mine Water Environ (in press)

Liu CP, Zheng CC (1994) Optimization estimation method of multiple types of hydrogeologic parameters (in Chinese). Geotech Invest Surv 2:33–37

Liu DG, Fei JG, Yu YJ (1980) A compilation of FORTRAN algorithms, vol 1 (in Chinese). Defense Industry Press, Beijing, pp 101–104

Xu SH, Zu XY (1999) Hydraulic capture technique for remedy of ground water contaminate by petroleum and its numerical model (in Chinese). J Hydraul Eng 1:71–76

Xue YQ, Xie CH, Wu JC (1991) A numerical model of the seawater intrusion in coastal aquifer. In: Xue YQ, Bear J (eds) Proceedings of international conference on modeling ground water flow and pollution. Nanjing University Press, Nanjing, pp 13–20

Xue YQ, Zhu XY, Wu JC (1986) Ground water dynamics (in Chinese). Geology Press, Beijing, pp 213–217

Yeh WWG (1981) On the computation of Galerkin velocity and mass balance: The finite element modeling of ground water flow. Water Resour Res 17:1529–1534

Yeh WWG (1986) Review of parameter identification procedures in ground water hydrology: the inverse problem. Water Resour Res 22:95–108